Arab J Sci Eng (2017) 42:4351–4364
DOI 10.1007/s13369-017-2438-x

RESEARCH ARTICLE - CHEMISTRY

Synthesis, Characterization, Electrical and Photocatalytic Studies of Polyacrylamide Zr(IV) Phosphosulphosalicylate, a Cation Exchanger: Its Application in the Removal of Hg (II) from Aqueous Solution

Seraj Anwar Ansari[1] · Fauzia Khan[1] · Anees Ahmad[1] · Waseem Raza[2] · Muneer Ahmad[2]

Received: 10 June 2016 / Accepted: 19 January 2017 / Published online: 14 February 2017

Abstract In this work, we synthesized successfully a new organic–inorganic material, polyacrylamide Zr(IV) phosphosulphosalicylate (PAAZPSS) by simple sol–gel method and converted in a cation exchanger and then applied as an adsorbent for the removal of Hg (II) from aqueous solution. In order to confirm the desired synthesis, the prepared material was characterized by many sophisticated techniques such as FTIR, SEM and XRD. The ion exchange adsorbent exhibits good ion exchange capacity (IEC) for alkali metal ion (K^+). Selective studies of this ion exchange adsorbent for different metal ions were performed, and on the basis of K_d values PAAZPSS was more selective for Hg (II). The sorption experiment for the Hg (II) removal was performed using batch method. The adsorption process followed Langmuir adsorption isotherm and pseudo-second-order kinetic model. The thermodynamic parameters revealed the feasibility, spontaneity, endothermic nature of the PAAZPSS-Hg (II) system. The material showed high value of dielectric constant, dielectric loss at low-frequency region and enhanced AC conductivity at low-frequency region so it can be used in energy storage devices. The material also showed good photocatalytic degradation of rhodamine B and crystal violet dyes. So it may be concluded that polyacrylamide Zr(IV) phosphosulphosalicylate can be employed not only for the treatment of inorganic metal ion and photocatalytic degradation of organic dyes but also in electrical application.

Keywords Sol–gel method · Adsorption isotherms · Kinetic and thermodynamics · Dielectric constant · Ac conductivity · Photocatalytic degradation

1 Introduction

Water pollution due to toxic mercury metal ions and its related compounds is a serious environmental concern. The major source of releasing mercury ions into drinking water is electrical and electronics manufacturing plants, erosion of natural deposits, release from refineries or factories and runoff from landfills or croplands, chloro-alkali plants, sulfide ore roasting operations and buttery industries [1,2]. Recently, impacts of human activity on heavy metal spread have been discussed [3]. Mercury has adverse effects on chromosomes, the central nervous system, pulmonary and kidney. At normal temperature and pressure, mercury exists in liquid state. The salt of mercury is mercurous (I) and mercuric (II); among these two forms, mercuric (II) is more common in environment and is soluble in water. The permissible contaminant limit for aquatic flora and fauna recommended by Tennessee Water Quality Control Board is 0.0014 mg L^{-1} [4]. It slowly bio-stores in the aquatic flora and fauna, reaching the human mainly through fishes and their prolonged consumption causes various neurological problems such as chest pain, labored breathing, vomiting, diarrhea, fever, metallic taste in the mouth and skin rash [5]. The chronic exposure may lead to tremors, limb weakness, anorexia, excessive shyness, irritability, headache and loss of memory. It has been reported that the exposure of developing fetuses and

✉ Anees Ahmad
aneesahmad.ch@amu.ac.in

1 Industrial Chemistry Research Laboratory, Department of Chemistry, AMU, Aligarh, India

2 Organic Chemistry Research Laboratory, Department of Chemistry, AMU, Aligarh, India

children below the age of four to mercury affects the normal development of brain. So, discharging of Hg and its related compounds into natural water bodies are serious concern for living beings and surroundings due to their high harmfulness, volatility and long persistence time; therefore, it is obligatory to remove mercury from wastewater before its recycle transport and discharge into the environment [6,7]. The applications of compositing or compost for soil bioremediation have been presented [8]. Seeing all the health and environmental hazards related to mercury ion and its compounds, it is obligatory to remove it from the waste water. Various chemical and physical methods such as adsorption, biological treatment, chemical precipitation, electrochemical treatment, fixed bed reactor, liquid membrane separation, oxidation and photochemical degradation are being employed for the removal of mercury. Among these adopted methods for the removal of mercury from aqueous solution, ion exchange followed by adsorption process was considered to be most suitable because of low-energy requirements, simplicity of design and probability of use again of the ion exchange adsorbent after regeneration for the removal of organic and inorganic pollutants from aqueous solutions [2]. The ion exchange resins as 'organic–inorganic' composite materials, e.g., poly-o-toluidine Zr(IV)tungstate composite [9], zirconium (IV) antimonotungstate [10], poly-ortho-toluidine Th(IV)molybdophosphate [11], polyacrylamide Zr(IV)iodate [12] and polyacrylamide chromium oxide [13], have been synthesized earlier by the integration of organic polymer into inorganic matrix by sol–gel mixing methods [14] . Recently, the synthesis and application of polymeric hybrid ion exchangers have also been discussed [15]. It has been reported that phosphate and Zr provide high exchange capacity, thermal stability, chemical stability, reproducibility, preferential ion selectivity and electrical conductivity to the material. Due to the aforementioned advantages, these materials gained wide applications as ion exchanger, catalyst [16], pollution controller, isolation of radioactive isotopes and in water treatment, which are of economic importance [11]. The main purposes of this work are:

1. Synthesis and characterization of polyacrylamide Zr(IV) phosphosulphosalicylate, to optimize the experimental condition (pH, amount of ion exchanger, and contact time) and to get maximum sorption capacity.
2. To study the adsorption isotherm, kinetics, and thermodynamics of Hg (II) sorption onto the surface of ion exchanger.
3. To measure electrical, dielectric property, AC conductivity, and the photocatalytic activity of the material for the degradation of organic pollutants.

2 Materials and Methods

2.1 Chemical Reagents and Instruments

The chemical reagents used for the synthesis of the ion exchanger material were $ZrOCl_2.8\,H_2O$, sulphosalicylic acid (Otto Chemie Pvt. Ltd., Mumbai, India), acrylamide (Otto Chemie Pvt. Ltd., Mumbai, India), and o-phosphoric acid (Merck, India). Rhodamine B (Rh B, $\lambda^{max} = 553$ nm) and crystal violet (CV, $\lambda^{max} = 588$ nm) were obtained from Sigma-Aldrich, India). All chemicals and reagents used in this work were of analytical grade. Stock solution of Hg (II) was prepared by dissolving appropriate amount of mercury salt in 1000-mL standard volumetric flask. Further required different metal ion concentrations were prepared by diluting the stock solution. A digital pH meter (Systronics μ pH system 361), FTIR spectrophotometer (Interspec 2020, Spectrolab, UK), an automatic thermal analyzer (DTG, 60 H Shimadzu), X-ray diffractometer (X' PRO-PANanalytical, Netherland), scanning electron microscope (JEOL JSM-6510 LV), a digital LCR meter (Pacific, PLCR 8C), photochemical reactor made of pyrex glass under UV light illumination, UV light intensity detector (Lutron UV-340), UV–Vis spectrophotometer λ-35 (Perkin Elmer) and a water bath incubator shaker were used.

2.2 Preparation of Polyacrylamide Zr(IV) phosphosulphosalicylate (PAAZPSS)

Polyacrylamide Zr(IV) phosphosulphosalicylate (PAAZPSS) hybrid organic–inorganic composite was prepared by modifying reported method elsewhere by adding equimolar aqueous solution of zirconium oxychloride drop-wise to aqueous solution of sulphosalicyclic acid, acrylamide and orthophosphoric acid with constant stirring at a temperature of 70±3 °C [17]. The pH of the mixture solution was maintained at 1 by adding 1M HNO_3. The gelatinous precipitate so formed was stirred at 70 °C for 8 h and kept in mother liquor for another 24 h. The gelatinous precipitate was filtered and washed with copious amount of distilled water to remove excess acid and dried in an oven at 50 °C. To obtain small granules, the hot dried material was immersed in sufficient amount of double distilled water and again dried at 50 °C. The dried material was converted in H^+ form by keeping it in 1M HNO_3 solution for 24 h with occasional shaking. After frequent washings with distilled water, excess acid from the material was removed and dried at 50 °C. The dried cation composite adsorbent was stored in desiccator for further use.

2.3 Chemical Stability Test

In order to confirm the chemically stability of polyacrylamide Zr(IV) phosphosulphosalicylate, it was immersed in different

concentrations of HCl, HNO_3, and NaOH. For this, 0.2g of material was kept in 20 mL of these solutions for 24 h.

2.4 Characterization of Cation Exchanger

In order to confirm the synthesis of composite and determination of the functional groups involved in the adsorption process, FTIR analysis of polyacrylamide Zr(IV)phosphosulphosalicylate was performed using the KBr disc method. The powder X-ray diffraction analysis was performed to know the nature of the ion exchange adsorbent by a PW-3050/60 diffractometer with Cu Kα radiation ($\alpha = 1.54$ Å). The surface morphology of the adsorbent material before and after the Hg (II) sorption on the surface of adsorbent was recorded with scanning electron microscope at various resolutions.

2.5 Ion Exchange Capacity

The ion exchange capacity (IEC) of the ion exchange material was determined by column method. For this, 0.5 g of the dry exchanger in H^+ form was packed into a glass tube of internal diameter of 0.8 cm with glass wool at its bottom. The column packed with ion exchange material was washed with distilled water to remove any excess acid which remained sticking on the granules. To determine IEC, 1.0 M solution of the respective metal nitrate was passed through the column at a pour speed of 1 mL min^{-1} till the effluent indicated the lack of H^+ ions. The effluent was collected and titrated with a standard solution of NaOH to determine the total H^+ ions released which is equal to the cation taken by the material [18].

2.6 Selective Studies

The distribution coefficient (K_d) values of cation exchanger for various metal ions under set condition were determined by batch method. For this, 0.2 g of ion exchange adsorbent in H^+ was treated with 20 ml of different metal salt solutions for 24 h with irregular shaking at room temperature to attain equilibrium. EDTA titration was used to determine the metal ion concentration before and after equilibrium. The K_d values were calculated by using the following Eq.

$$K_d = \frac{(\text{mmoles of metal ions in exchanger phase}) \times (\text{Total vol.of solution})}{(\text{mmoles of metal ions in solution phase}) \times (\text{Weight of exchanger})} \quad (1)$$

2.7 Batch Adsorption Experiments

Adsorption experiments were performed in batch mode using 100-mL conical flask equipped with stopper to avoid variation in concentration due to evaporation. For this, 0.2 g exchanger in H^+ form in 20 mL of 0.01 M metal ion solution was equilibrated on a shaker incubator at constant temperature at a speed of 80 rpm for a given time. The ion exchange adsorbent was separated from the solution by filtration through Whatman-42 filter paper, and residual metal ion concentration was determined by titration against 0.001 M EDTA solution. Further, all the experiments were carried out at varying conditions of contact time, dose effect, initial concentration, pH and temperature. The retained quantity of metal ion in the ion exchange phase is determined by Eqs. (2) and (3), respectively:

$$q_e = \frac{(C_0 - C_e) \times V}{m} \quad (2)$$

$$\%\text{metal adsorbed} = \frac{100 \times (C_0 - C_e)}{C_0} \quad (3)$$

where C_0 and C_e are the initial and equilibrium concentration of metal ion in the solution expressed in mg L^{-1}, respectively, V is the volume of the metal solution in Liter and m is the amount of ion exchanger adsorbent in g.

2.8 Adsorption Isotherms

The relationship between the amount of metal adsorbed and the concentration of metal ion may be described by the adsorption isotherm. The experimental data were fitted to Langmuir, Freundlich, and Temkin isotherm models to establish the most appropriate model for the PAAZPSS-Hg (II) system sorption.

The Langmuir equation can be expressed by Eq. (4) [19].

$$\frac{1}{q_e} = \left(\frac{1}{K_L.q_m}\right)\frac{1}{C_e} + \frac{1}{q_m} \quad (4)$$

where C_e is the equilibrium concentration of the adsorbate in solution phase in mg L^{-1} and q_e is the amount adsorbed per unit mass of adsorbent in mg g^{-1}; q_m is maximum adsorption capacity in mg g^{-1}; K_L is the Langmuir isotherm constant which presents the energy of adsorption in L mg^{-1}.

The equilibrium dimensionless parameter, R_L, was further used to evaluate the favorability of the Langmuir model and written by Eq. (5) [20]:

$$R_L = \frac{1}{1 + bC_0} \quad (5)$$

where C_0 is the highest initial concentration of metal ion in mgL^{-1}, and b is the Langmuir constant. The value of R_L determines the shape of isotherm as if: $R_L > 1$ (unfavorable), $R_L = 1$ (linear) and $R_L > 0 < 1$ (favorable).

The linear form of Freundlich equation can be expressed by Eq. (6) [21]:

$$\ln q_e = \ln K_F + \frac{1}{n_f} \ln C_e \tag{6}$$

where K_F and $\frac{1}{n}$ are Freundlich constants representing adsorption capacity and intensity of adsorption in the adsorption process, respectively. The value of $\frac{1}{n_f}$ for a favorable adsorption condition should be less than 1[22, 23]. The larger value of n_f indicating the system is more heterogeneous [24,25]. Freundlich isotherm model was not followed in this work because the value of $\frac{1}{n_f}$ is greater than 1.

According to Temkin adsorption isotherm model, the heat of adsorption of all the molecules in the layer would decrease linearly rather than logarithmically because of adsorbent–adsorbate interaction. The Temkin isotherm can be expressed by Eqs. (7) and (8), respectively [26,27].

$$q_e = B \ln A + B \ln C_e \tag{7}$$

and;

$$B = \frac{RT}{b} \tag{8}$$

where b is the Temkin constant related to heat of adsorption in $Jmol^{-1}$, T is the absolute temperature in Kelvin, R is the universal gas constant in Lg^{-1} and equal to 8.314 $Jmol^{-1}K^{-1}$ and A is Temkin isotherm constant or equilibrium binding constant in Lg^{-1}.

2.9 Adsorption Kinetics

The mechanism of sorption process was determined by applying the experimental data to the Lagergren' pseudo-first-order, Ho and Mckay' pseudo-second-order, and Weber' intraparticle diffusion models. The general expression of Lagergren' pseudo-first-order can be expressed by the following Eq. (9) [21,22,28]:

$$\frac{\partial q_t}{\partial t} = K_{0,1} (q_e - q_t) \tag{9}$$

where $K_{0,1}$ is the pseudo-first-order rate constant expressed in min^{-1}, q_e and q_t are adsorption capacities in mgg^{-1} at equilibrium and at time t in min, respectively.

Integrating and taking log of Eq. (9) under the condition $q_t = 0$, at $t = 0$ and $q_t = q_t$ at $t = t$ yield Eq. (10):

$$\log (q_e - q_t) = \log q_e - \frac{K_{0,1}}{2.303} t \tag{10}$$

The pseudo-second-order kinetics model can be written by Eq. (11) [21,29]:

$$\frac{\partial q_t}{\partial t} = K_{0,2} (q_e - q_t)^2 \tag{11}$$

where $K_{0,2}$ is the pseudo-second-order rate constant expressed in $gmg^{-1}min^{-1}$, q_e and q_t are adsorption capacities in mgg^{-1} at equilibrium and at time t in min, respectively. Integrating Eq. (10) under the condition $q_t = 0$, at $t = 0$ and $q_t = q_t$ at $t = t$, yields Eq. (12):

$$\frac{t}{q_t} = \frac{1}{K_{0,2} q_e^2} + \frac{t}{q_e} \tag{12}$$

In the adsorption process, the migration of solute from the bulk of solution to the surface of the adsorbent does not takes place in a single step. The extent of adsorption can be related to intraparticle diffusion and may be written by Eq. (13) [30]:

$$q_t = K_{id} t^{1/2} + C \tag{13}$$

where K_{id} is the intraparticle diffusion constant expressed in $mgg^{-1}min^{0.5}$, C is the intercept expressed in mgg^{-1} reflects the boundary layer effect [31].

2.10 Thermodynamic Studies

Thermodynamic parameters such as change in enthalpy ($\Delta H°$), entropy ($\Delta S°$) and Gibb's free change ($\Delta G°$) were determined using the following Eq. (14) [32]:

$$\Delta G° = -RT \ln K_d \tag{14}$$

where R is the universal gas constant equal to 8.314 $Jmol^{-1}$ K^{-1}, T is absolute temperature expressed in Kelvin, and K_d is the equilibrium constant and equal to $\frac{q_e}{C_e}$. Similarly, the ($\Delta H°$) and ($\Delta S°$) are calculated using the following Eq. (15):

$$\ln K_d = \frac{\Delta S°}{R} - \frac{\Delta H°}{RT} \tag{15}$$

2.11 Dielectric Constant, Loss Tangent and AC Conductivity Measurements

A digital LCR meter (Pacific, PLCR 8C) was used to measure the electrical, dielectric, and AC conductivity of the ion exchange composite. For this, the samples of the ion exchange composite were pelletized by pressing under a hydraulic pressure of 25 kN for 3 min and then applying a conductive silver paste to form the electrodes in contact with the two circular faces. The measurements were taken at room temperature (25 ± 2 °C) in the frequency range of 75–5 MHz. The variation of dielectric constant irrespective

Table 1 Ion exchange capacity (IEC) of polyacrylamide Zr(IV) phosphosulphosalicylate for monovalent and bivalent metal ions

Metal ions	0.1 M solution of metal salts	Ionic radii (A^0)	Hydrated radii (A^0)	Ion exchange capacity meq/g dry exchanger
Na^+	$NaNO_3$	0.97	7.90	1.72
K^+	KNO_3	1.33	5.30	2.44
Mg^{2+}	$MgCl_2$	0.78	10.80	1.04

of applied frequency in solids mainly depends on intrinsic electric dipole polarization and interfacial polarization. The dielectric constant of a material can be represented by Eq. (16):

$$\varepsilon' = \frac{C_p t}{\varepsilon_o A} \tag{16}$$

The imaginary part of the dielectric constant can be obtained by Eq. (17):

$$\varepsilon'' = \varepsilon' \tan \delta \tag{17}$$

where $\tan \delta$ is called as the dielectric loss tangent, which is proportional to the loss of energy dissipated as heat from the applied field into the sample.

The AC electrical conductivity of the sample was calculated by using Eq. (18):

$$\sigma_{AC} = 2 \pi f \varepsilon'' \varepsilon_0 \tag{18}$$

2.12 Photocatalytic Experiment

The photocatalytic oxidation of rhodamine B (RhB, λ_{max} = 553 nm) and crystal violet (CV, λ_{max} = 588 nm) dyes was done by using an immersion well photochemical reactor made of Pyrex glass under UV light illumination. The UV light source was a 125-W medium pressure mercury lamp. During all the experiments, the temperature of aqueous solution of dyes was maintained around (20 ± 0.5 0C) by refrigerated water circulation to prevent the heat from the solution and radiation emit by the UV lamp (IR and short wavelength). The radiation intensity falling on the solution was measured using UV light intensity detector (Lutron UV-340) and found to be 2.58 mW/cm^2. The polyacrylamide Zr(IV) phosphosulphosalicylate (0.2 g, 1 g/L) was dispersed in 200 ml of prepared aqueous solution of dye into the photoreactor. Prior to illumination, the suspension was first sonicated for 15 min and then magnetically stirred for 15 min in dark to achieve adsorption–desorption equilibrium. During irradiation, the reaction sample was periodically sampled (5 mL) and centrifuged to remove the powder. A blank experiment was also done for degradation of rhodamine B of concentration 10 ppm (0.020 mmoles) and crystal violet aqueous solution of 10 ppm (0.024 mmoles) without catalyst under UV light illumination. The photocatalytic degradation of rhodamine B and crystal violet was monitored by using PerkinElmer spectrophotometer (λ = 35) at their λ_{max} = 553 and 588 nm, respectively [33]. The degradation efficiency of dyes was calculated by using Eq. (19):

$$\text{Degradation}\% = \frac{C_0 - C_t}{C_0} \times 100\% \tag{19}$$

where C_0 is initial concentration and C_t is concentration at particular time (t).

3 Results and Discussion

In the current study, an effort has been made to synthesize the polyacrylamide Zr(IV) phosphosulphosalicylate ion exchanger and its application for the removal of Hg (II) from synthetic solution, and its electrical and photocatalytic properties were also explored. The column process was used to determine the ion exchange capacity of the hybrid cation exchanger for alkali and alkaline earth metal ions, and results are listed in Table 1. It is obvious that the ion exchange capacity increases with a decrease in hydrated ionic radii. Similar observations were also reported for the exchange of alkali and alkaline earth metal ions on zirconium (IV) arsenate vanadate [13,34]. The polyacrylamide Zr(IV) phosphosulphosalicylate cation exchanger followed the IEC order, $K^+ > Na^+ > Mg^{2+}$. The maximum IEC was found to be 2.44 meq per dry weight of the cation exchanger for the K^+. It was observed that the material was quite stable in 1M HNO_3, 1M HCl, 0.5M H_2SO_4 and 0.1M NaOH. In order to explore the potential ability of the polyacrylamide Zr(IV) phosphosulphosalicylate in the separation of metal ions, the distribution coefficient values for some metal ions were evaluated in distilled water. The results are listed in Table 2. On the basis of K_d results of the present investigation, it may be concluded that the polyacrylamide Zr(IV) phosphosulphosalicylate has a hopeful capability for the sorption of Hg (II) from the aqueous solution. The K_d values of Hg(II) are much higher than the K_d values of other metal ions, thus showing it to be a highly selective sorbent material for Hg(II). Chemical stability is an important parameter for the suitability of ion exchange materials for analytical applications. In

Table 2 Distribution coefficient (K_d) values of metal ions on polyacrylamide Zr(IV) phosphosulphosalicylate in DMW

Metal Ion	K_d
Co^{2+}	6.06
Cd^{2+}	10.73
Ni^{2+}	11.11
Mg^{2+}	16.27
Zn^{2+}	27.27
Pb^{2+}	34.21
Cu^{2+}	100.11
Hg^{2+}	328.88

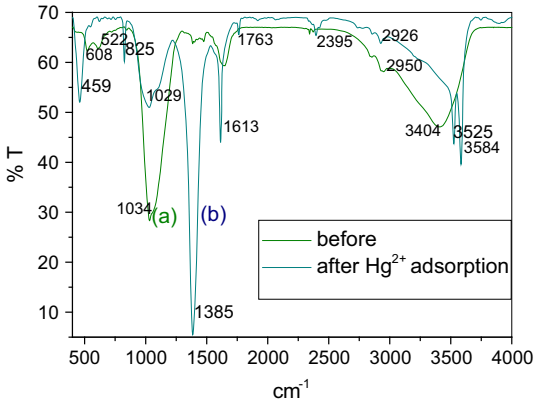

Fig. 1 **FTIR** spectra of polyacrylamide Zr (IV) phosphosulphosalicylate composite (**a**) and after the Hg (II) adsorption onto polyacrylamide Zr (IV) phosphosulphosalicylate (**b**)

view of this, the chemical stability of polyacrylamide Zr(IV) phosphosulphosalicylate has been evaluated in one mole concentrations of HCl, HNO_3, H_2SO_4, and NaOH. It was found that the material is fairly stable in these solutions.

3.1 FTIR Analysis

The FTIR spectra of polyacrylamide Zr(IV) phosphosulphosalicylate ion exchange adsorbent before and after Hg (II) adsorption on the surface are shown in Fig. 1. Functional groups taking part in the adsorption process are shown in Fig. 1a. A broad peak at 3404.28 cm^{-1} may be assigned due to stretching of -OH or –NH of amide group. A sharp and intense peak at 1616.73 cm^{-1} may be attributed to the C=O group stretching of sulfosalicylate molecule [35,36]. In the spectrum, band at 1477.04 cm^{-1} and 1434.55 cm^{-1} may be assigned to carbonate group and benzene ring. The peak appeared at 1384 cm^{-1} may be assigned for the presence of considerable amount of acrylamide in the composite [35]. Peak at 1034 cm^{-1} may attribute to symmetric stretching vibration of the $–SO_3$ of sulfonic acid salt. Two sharp peaks at 608.16 cm^{-1} and 521.30 cm^{-1} may be assigned to metal–oxygen linkage occurring through polymerization. Figure 1b shows the visible changes in the position, and frequency of peaks 521, 608, and 806 cm^{-1} was observed at 459, 620, and 825 cm^{-1} after sorption of Hg (II) onto the surface of ion exchanger. Figure 2 shows the SEM images of polyacrylamide Zr(IV) phosphosulphosalicylate at different magnifications before and after the Hg (II) adsorption. It was very obvious from Fig. 2a–2c that the surface of cation exchanger is sufficiently rough and irregular and that from Fig. 2a'–c' it was remarkably modified after the Hg (II) adsorption onto the surface of ion exchanger. The irregular surface of material provides suitable binding sites for the adsorption of Hg (II) over its surface through ion exchange mechanism. The XRD pattern of polyacrylamide Zr(IV) phosphosulphosalicylate cation exchanger (Fig. 3) with and without adsorption of Hg(II) indicated amorphous nature.

3.2 Batch Adsorption Experiments

3.2.1 Effect of Contact Time

In order to see the effect of contact time on the adsorption of Hg (II), batch experiment was done using 0.2 g ion exchanger at 30 °C and neutral pH over the contact time range from 5 to 180 min. Figure 4a shows the relation between quantity of Hg (II) adsorbed at particular time and contact time. It revealed that at initial stage rate of adsorption is rapid and thereafter decreases gradually with time until adsorption reached at equilibrium point, i.e., 80 min. The reason for this trend is due to the adsorption of Hg (II) on the exterior surface of ion exchange adsorbent at the initial stage of contact time. The adsorption process reached at equilibrium point as the exterior surface gets exhausted by Hg (II) after that it was diffused into pores and adsorbed by the interior surface of the ion exchange adsorbent. After that it becomes constant, and further no increase in adsorptive removal efficiency with increase in time was observed. Therefore, 80 min was chosen as equilibrium time for the adsorption system.

3.2.2 Effect of Adsorbent Dose

The dependence of dose of ion exchange adsorbent on Hg (II) adsorption was studied with different amounts varying from 0.02 to 3g into 20 ml of 0.01M Hg (II) solution at neutral pH. It is obvious from Fig. 4b that with increasing the dose of ion exchange adsorbent % adsorption removal also increases, reaching the maximum value with an increase in amount from 0.02 to 0.15 g, but beyond this value the percent adsorptive removal of Hg (II) reached almost a constant value. This is because the number of adsorbent particles increases with increase in the amount of ion exchange adsorbent, resulting in increased number of active adsorption sites, and thus, more Hg (II) can be attached to the surface of ion exchanger.

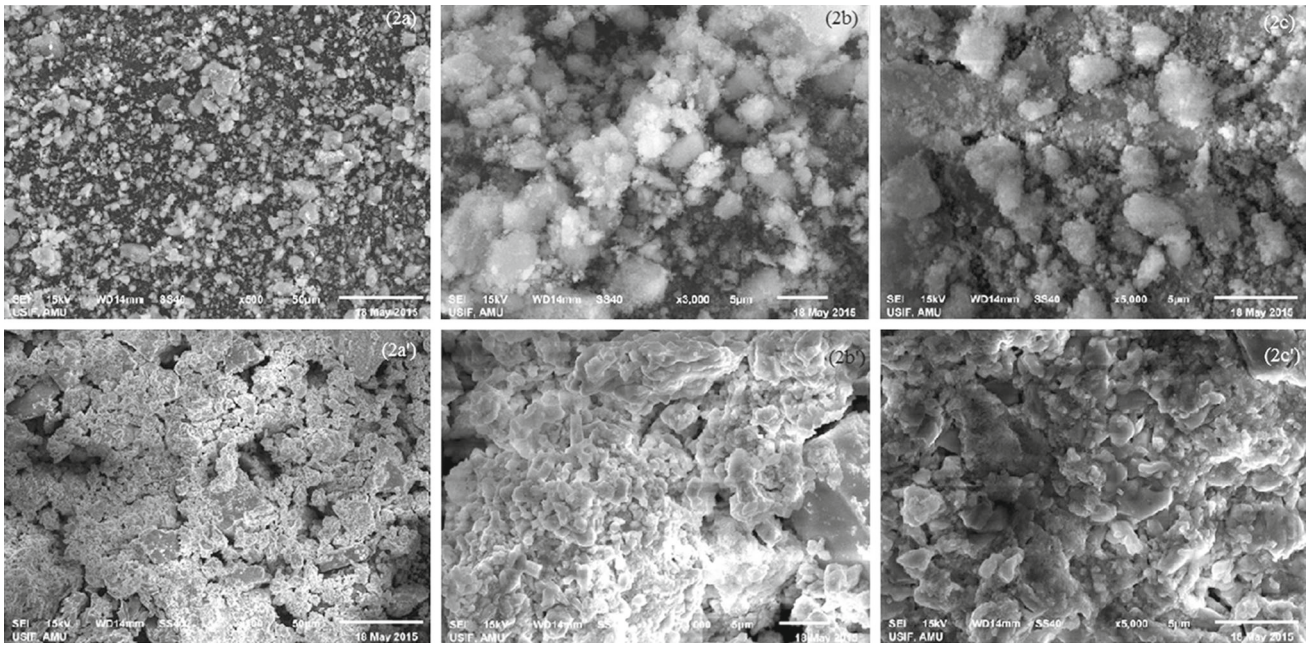

Fig. 2 SEM images of polyacrylamide Zr(IV) phosphosulphosalicylate composite (2a–c), and Hg(II) loaded polyacrylamide Zr(IV) phosphosulphosalicylate composite (2a'–2c') at different resolutions

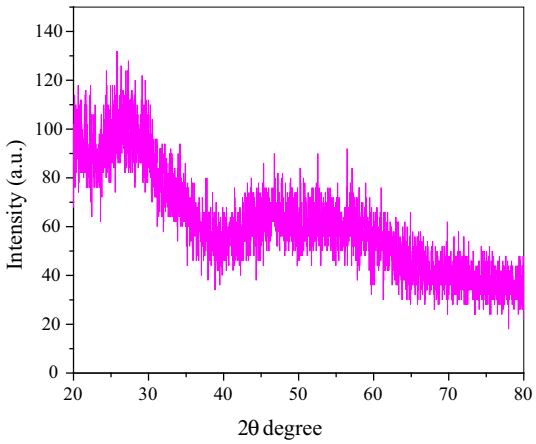

Fig. 3 XRD of polyacrylamide Zr(IV) phosphosulphosalicylate loaded with Hg (II)

The maximum adsorptive removal was observed at 0.15 g of adsorbent dose; therefore, it was selected for further experiment.

3.2.3 Effect of pH

The pH of the adsorbate solution plays an important role in the adsorption of adsorbate. On increasing or decreasing the acidity or alkalinity of the working solution, the property of adsorbate solution may change due to the surface charge on the adsorbent. Therefore, the effect of pH of solution on the uptake of Hg (II) was studied in batch method over the pH range of 1–10. The pH of working solution was maintained by adding HNO_3 or NaOH solution. For this, 0.2 g of ion exchanger in 20 mL of 0.01M Hg (II) was agitated at 30°C in orbital water bath shaker at 120 rpm for predetermined time. Figure 4c shows the relation between pH and quantity adsorbed onto the surface of ion exchanger; it may be said that at more acidic condition, the adsorption capacity is lower. By further increasing the pH of the solution, the sorption capacity also increases, reaching the maximum value, after that it becomes almost constant; this is because at low pH, H^+ are present relatively in large amount in the solution which compete with Hg (II) ions for adsorption sites of the polyacrylamide Zr(IV) phosphosulphosalicylate. The removal of Hg (II) is mainly due to adsorption, which is partly attributed to ion exchange between Hg^{2+} and H^+ ions on the adsorbent surface. The pH of the solution before and after Hg (II) ions adsorption decreased from 3.9 to 3.3. This trend was found because the exchanged H^+ ions are released to the solution, resulting in the lowering of pH values. The adsorption process followed by ion exchange can be expressed by Eq. (20):

$$2R - H^+ + Hg^{2+} \longrightarrow R_2Hg^{2+} + 2\,H^+ \tag{20}$$

3.2.4 Effect of Initial Concentration

The initial concentration of adsorbate solution plays an important role in the rate of adsorption. In total, 0.002–0.014 M initial concentration was studied on the uptake of

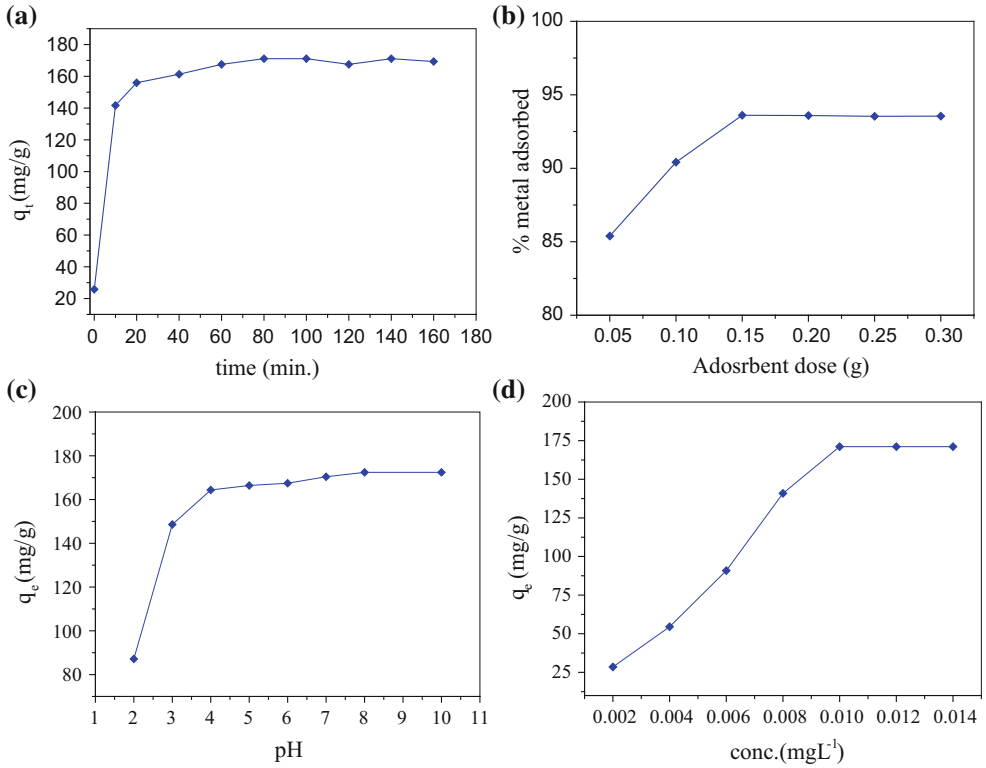

Fig. 4 Effect of contact time (**a**), effect of adsorbent dose (**b**), effect of pH (**c**), effect of concentration (**d**) on adsorption of Hg(II) onto the polyacrylamide Zr(IV) phosphosulphosalicylate

Hg (II) by polyacrylamide Zr(IV) phosphosulphosalicylate under the set experimental condition. It is understood from Fig. 4d, the adsorption capacity increases with increase in initial Hg (II) ion concentration, reaches to a maximum and after that attained a constant value, further there is no increment in adsorptive removal capacity, this trend was observed because of increased concentration gradient act as an enhanced driving force which disables the resistance to mass transfer of Hg (II) ion between aqueous phase and solid phase.

3.2.5 Adsorption Isotherms

Figure 5a plots between $\frac{1}{q_e}$ vs. $\frac{1}{C_e}$, which gives a straight line with slope $\left(\frac{1}{q_m K_L}\right)$ and intercept$\left(\frac{1}{q_m}\right)$. Langmuir parameters and correlation coefficients calculated from isotherm are given in Table 3. The maximum monolayer adsorption capacity was found to be 188.6 mg/g, which is very close to the experimental value. Therefore, it may be said that the adsorption of Hg (II) ion was favored by Langmuir adsorption isotherm. From Table 3, the value of R_L falls between 0 and 1, confirming the favorability of Hg (II) adsorption onto polyacrylamide Zr(IV) phosphosulphosalicylate. R_L values are lower for higher Hg (II) concentrations, and adsorption is therefore more favorable. The Temkin constants b and A were calculated from the slopes (B) and intercepts (B ln A) of Fig. 5c, respectively. The Temkin isotherm constant A was found to be 564.9105 Lg^{-1}, which indicates higher polyacrylamide Zr(IV) phosphosulphosalicylate- Hg (II) potential. The Temkin constant b was found to be 0.0054 Jmol^{-1}, indicating a weak interaction between the polyacrylamide Zr(IV) phosphosulphosalicylate- Hg (II) potential which favors the physical adsorption [21,27,37].

3.2.6 Adsorption Kinetics

Figure 6a shows the relation log $(q_e - q_t)$ vs. t. The adsorption rate constant for pseudo-first-order, $K_{0,1}$ and q_e can be calculated from the slopes and intercepts of the plots. The slopes and intercepts of Fig. 6b give the value of $K_{0,2}$ and $q_e{}^{cal}$, respectively. The quantity of Hg^{2+} ions adsorbed was calculated from the model found to be 172.4 mg g^{-1}, which is very close to experimental value that favors the pseudo-2^0-order kinetic model. Since pseudo-second-order kinetic model was followed in this experiment, other were rejected and not mentioned. So among the various kinetics models parameter calculated from the corresponding plots, only pseudo-second-order data are presented in Table 4.

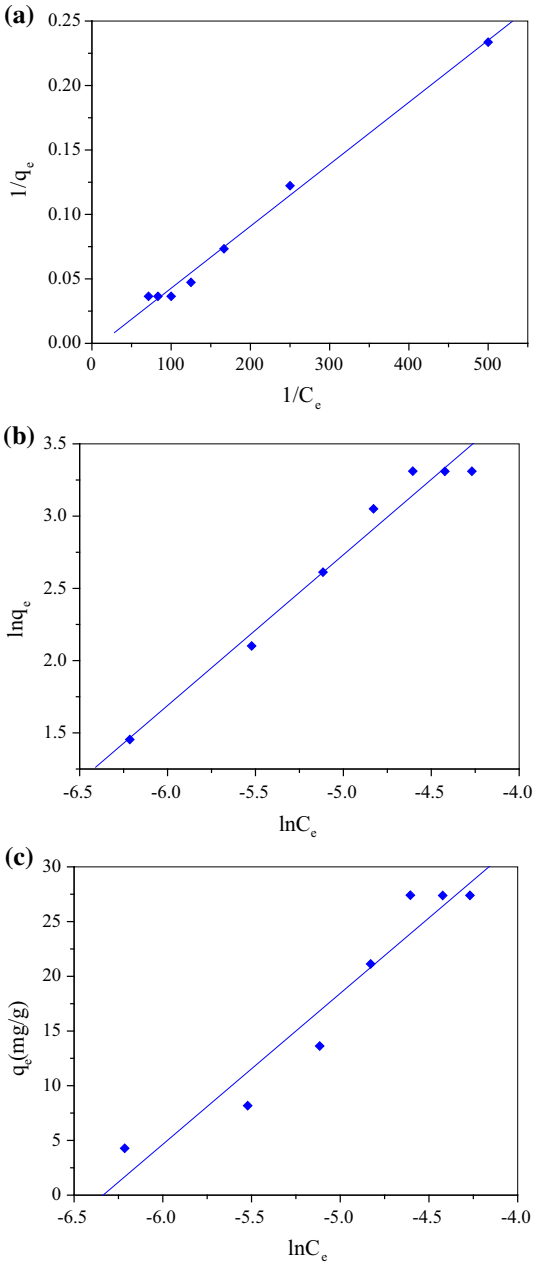

Fig. 5 Adsorption isotherms models (**a**) Langmuir (**b**) Freundlich, and (**c**) Temkin

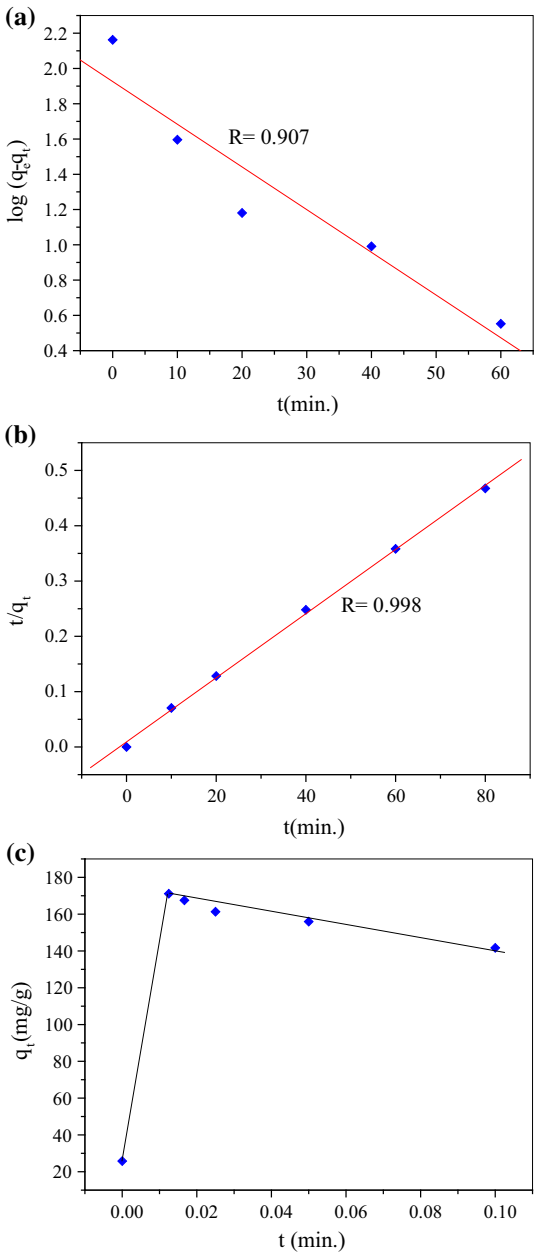

Fig. 6 Kinetic isotherm models (**a**), Lagergren pseudo-first-order **(b)**, Ho and McKay' pseudo-second-order **(c)**. Weber's intraparticle diffusion model

Table 3 Isotherm parameters for adsorption of Hg (II) onto polyacrylamide Zr (IV) phosphosulphosalicylate

Adsorption system	q_e^{exp}	Langmuir isotherm parameters			
		q_e^{max}	b	R_L	R^2
PAMZPSS-Hg(II)	171.0916	188.6792	0.0005	0.9999	0.9934

3.2.7 Thermodynamic Studies

The adsorption capacity of an ion exchange adsorbent is influenced by temperature. The effect of temperature on adsorption was studied in batch method at different temperatures 303, 313, and 323 K for polyacrylamide Zr(IV) phosphosulphosalicylate- Hg (II) system. It was found that the adsorption capacity decreases from 171 mgg^{-1} – 71 mgg^{-1} with increase in the temperature from 303 to 323 of the system solution, indicating that the adsorption process was endothermic in nature. The reason for this trend is with increasing temperature, the attractive forces between cation exchange adsorbent and Hg (II) are deteriorated and so the sorption decreases. And also at higher temperature, the thickness of boundary layer shrinks due to the rise in affinity

Table 4 Kinetic parameters for adsorption of Hg (II) onto polyacrylamide Zr (IV) phosphosulphosalicylate

Adsorption system	q_e^{exp}	Pseudo-second-order		
		q_e^{cal}	$K_{0,2}$	R^2
PAMZPSS-Hg(II)	171.0916	172.4137	0.0064	0.9996

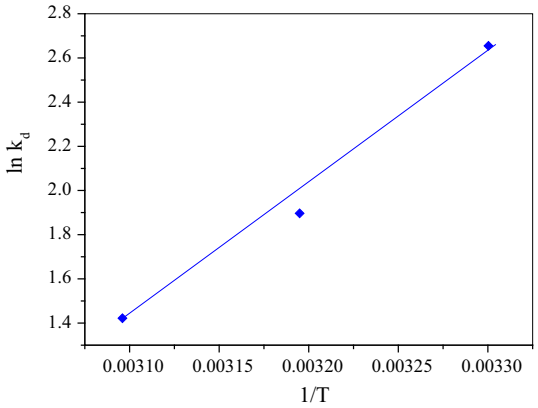

Fig. 7 Effect of temperature on the adsorption of Hg(II) on the surface of polyacrylamide-Zr(IV)-sulphosalicylate

of the Hg (II) ions to outflow from the adsorbent surface to the solution phase, which also results in decrease in adsorption with increase in temperature. Therefore, on the basis of adsorption capacities obtained at various temperatures, it may be concluded that the lower temperature favors the Hg (II) ions adsorption on the surface of adsorbent exchanger. Figure 7 shows the relation between ln K_d vs. $\frac{1}{T}$ and the value the ΔH° expressed in kJmol^{-1}, and ΔS° in Jmol$^{-1}K^{-1}$, were obtained from the slope and intercept of the plot. The value of various thermodynamic parameters calculated for Hg (II) adsorption on the surface of polyacrylamide Zr(IV) phosphosulphosalicylate is listed in Table 5, showing that the value of change in Gibb's free energy change (ΔG°) becomes more positive with increasing the temperature of the system solution. This indicates that the adsorption for Hg (II) on PAMZPSS is more favored at low temperature, and the value of (ΔG°) remains negative at all temperatures that confirm the feasibility and spontaneity of the sorption process. Sine, the calculated value (ΔG°) was found to be less than -20 kJ mol^{-1} come under physiosorption that mean involves the electrostatic interaction between surface sites and Hg (II) ions [21]. It was found that adsorption capacity of the PAMZPSS for Hg (II) decreases with increasing temperature. The positive value of the standard enthalpy change (ΔS°) indicated that the ion exchange process was endothermic in nature. In our result, the value of ΔS° was found >10 Jmol$^{-1}K^{-1}$, following an associative mechanism, and there was no important modification in the internal structure of the ion exchange adsorbent [38].

Table 5 Thermodynamic parameters for adsorption of Hg (II) onto polyacrylamide Zr (IV) phosphosulphosalicylate

Adsorption system	ΔG° (kJ/mol)			ΔH° (kJ/mol)	ΔS° (J/mol/K)
	303 K	313 K	323 K		
PAMZPSS-Hg(II)	−6.6875	−4.7775	−3.5822	6.0449	−17.3350

3.2.8 Dielectric Constant, Loss Tangent and AC Conductivity

Figure 8 shows the logarithmic plots of real (Fig. 8a) and imaginary parts of dielectric constants (Fig. 8b) versus applied frequency for the composite at 30°C. Plots revealed the high value of dielectric constant atx low-frequency region, because of the electrode–electrolyte interface polarization (i.e., Maxwell–Wagner–Sillar polarization). With an increase in frequency, the oscillating charge carriers may not able to contribute significantly to the dielectric constant owing to the high periodical reversal of field. Therefore, dielectric constant of the sample decreases with increasing frequency, which is a typical behavior of normal ion conducting materials [39–41]. The variation of $tan\ \delta$ as a function of applied frequency (Fig. 8c) at 30°C shows that dielectric loss rapidly decreases with increase in frequency and the single relaxation peak in the spectrum. The relaxation peak in the spectrum might be due to polyacrylamide in the composite. The variation in AC conductivity with frequency (Fig. 8d) for the sample at 30°C revealed that conductivity of the sample increases gradually with the increase in frequency. The conductivity enhancement of the composite may be due to the increased charge carriers and easier formation of the conducting network through better inter-particle contact among the charge carriers [42,43].

3.2.9 Evaluation of Photocatalytic Performance

The photocatalytic efficiency of the polyacrylamide Zr(IV) phosphosulphosalicylate was investigated by monitoring the photodegradation of two different model dyes such as rhodamine blue (RhB) and crystal violet (CV) dyes in aqueous medium under UV light illumination. The controlled experiment showed that RhB and CV were resistant to degradation during UV light irradiation without photocatalyst. However, some degradation of dyes takes in dark in the presence of polyacrylamide Zr(IV) phosphosulphosalicylate due to adsorption of dyes on the surface of catalysts. Figure 9a and b reveals that the peaks associated with maximum wavelength absorbance of both dyes (λ^{max} for rhodamine B = 553 nm and λ^{max} for crystal violet = 588 nm) decrease gradually as irradiation time increases, and the corresponding color of solution became lighter and lighter as the time increases due to break-

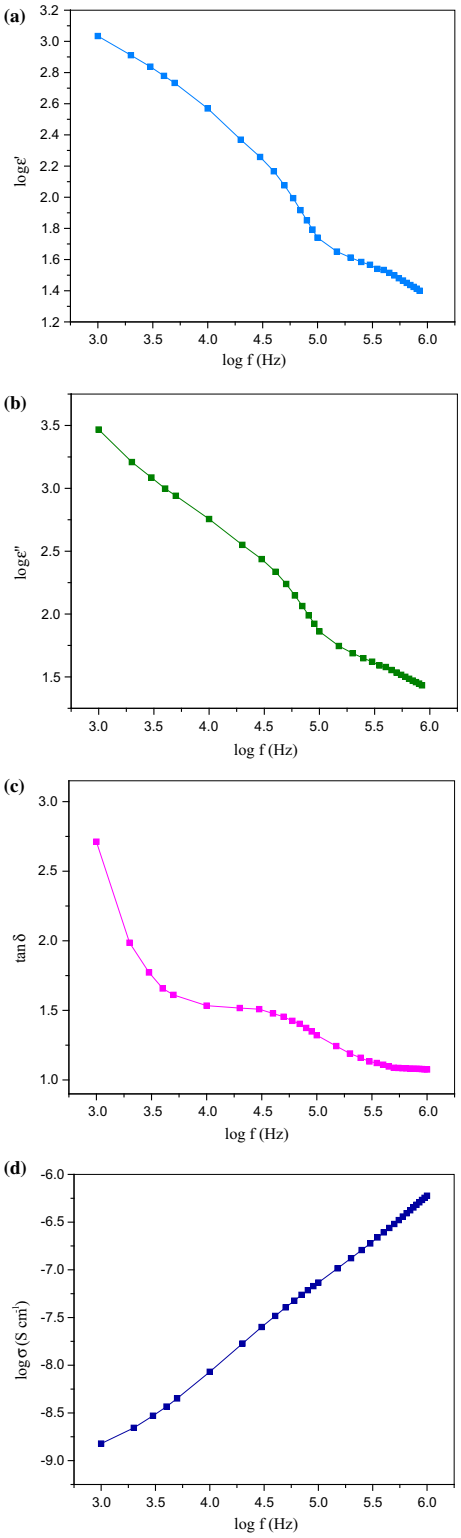

Fig. 8 **(a)** Plot of real part of the dielectric constant with frequency at room temperature. **(b)** Plot of imaginary part of the dielectric constant with frequency at room temperature. **(c)** Plot of dielectric loss with frequency at room temperature. **(d)** Variation of logarithmic AC conductivity with frequency at room temperature

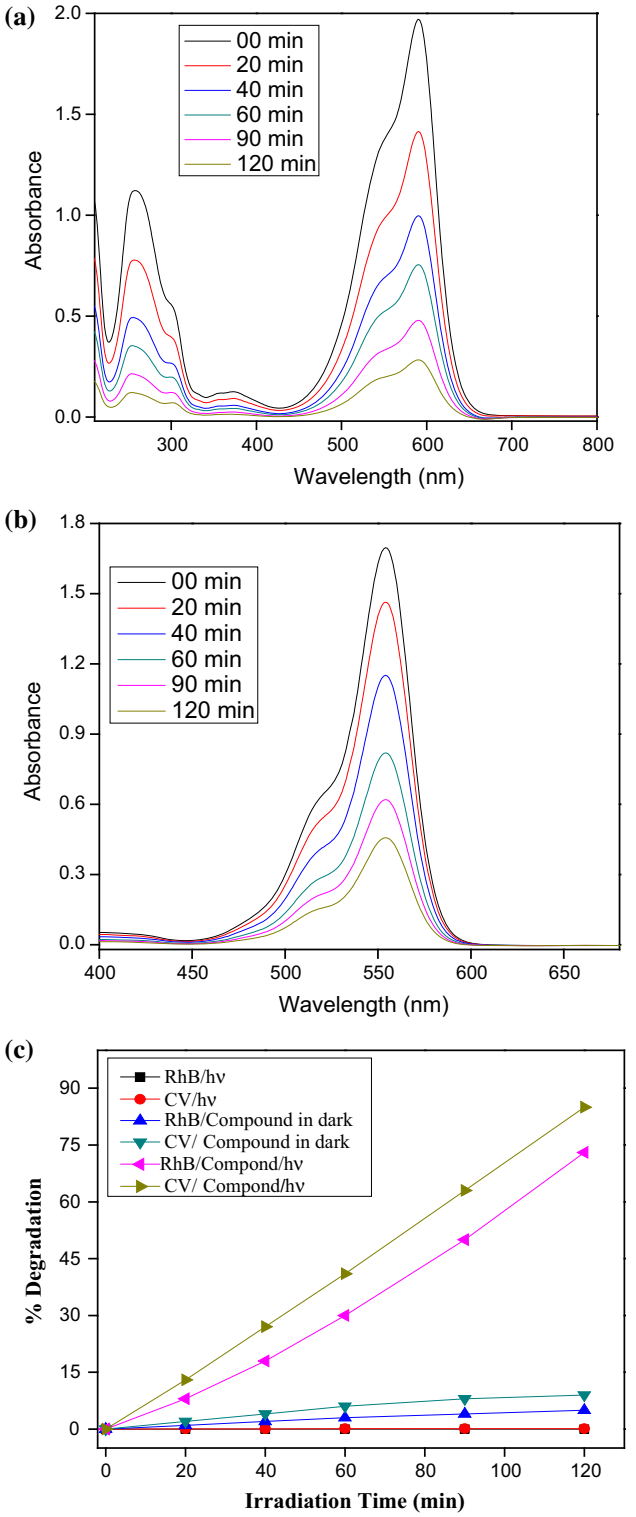

Fig. 9 Degradation of CV (**a**) and RhB (**b**) dyes, respectively, at different time intervals in the presence of synthesizes material. **(c)** Percentage degradation of RhB and CV dyes in aqueous solution as a function of time in the presence and absence of fabricated photocatalyst and in the presence and absence of UV light

Table 6 Comparison of Hg(II) sorption capacity of polyacrylamide Zr(IV) phosphosulphosalicylate with different adsorbents

S.no.	Adsorbents	q^{max} (mgg^1)	References
1	Graphene oxide/Fe-Mn composite	32.9	[47]
2	Amino and thiolated multi-walled carbon nanotubes	204.64	[48]
3	Chemically functionalized silica gel with alkynyl-terminated monolayers	171.48	[49]
4	Polypyrrole/SBA-15 nanocomposite	200	[50]
5	Thiourea-functionalized chelating fiber	52.04	[51]
6	Thiol-functionalized graphene oxide	107.52	[52]
7	Thymine-grafted reduced graphene oxide	142	[53]
8	Polyacrylamide Zr(IV) phosphosulphosalicylate	188.6	This study

ing of chromophoric group present in dyes [44,45]. It is very clear from Fig. 9c that 85 and 73 % degradation of dyes takes place after 120-min irradiation, revealing that the degradation of RhB was found to be lower than CV because of the presence of stable and bulky aromatic rings that suppress the interaction between catalysts and dye [46]. The adsorption of RhB was lower than CV on the surface of catalysts that decrease the photocatalytic degradation of RhB. The percentage degradation of dyes under UV light illumination is shown in Fig. 9c. The degradation comparison between two dyes was also made on mass basis; the mass of RhB and CV is of 479.01 and 407.98, respectively. Therefore, the degradation of CV was higher than RhB because of lower mass.

The comparison of Langmuir's maximum monolayer adsorption capacity (mgg^{-1}) for Hg (II) on various adsorbents is given in Table 6. Therefore, it may be concluded that polyacrylamide Zr(IV) phosphosulphosalicylate showed better adsorption capacity than many other adsorbents.

4 Conclusion

In this study, we have synthesized successfully a new ion exchanger, polyacrylamide Zr(IV) phosphosulphosalicylate highly effective and highly efficient for the removal of Hg (II) from aqueous solution. The material shows a good ion exchange capacity 2.44 meq per gram of dry material for K^+ and high K_d value 348 mL/g for Hg (II), respectively. The ion exchange adsorbent was fairly stable in acids and bases (HCl, HNO_3, and NaOH). The optimum condition for maximum adsorptive removal of Hg (II) from aqueous solution was found to be 0.01 M of Hg (II) concentration, adsorbent dose 0.15g, contact time 80 min, and pH 7.0. The adsorption equilibrium time for the PAAZPSS-Hg (II) adsorption system was 80 min. The experimental adsorption capacity is very close to calculated value obtained from these models. On the basis of these results and high value of regression coefficient, the adsorption system for PAAZPSS-Hg followed Langmuir adsorption isotherm and pseudo-second-order kinetic. The maximum Langmuir adsorption capacity was found to be 188.67 mgg^{-1} with dimensionless constant value less than 1 and greater than 0. The negative value of $\Delta G°$ (-3.5822- and -6.6875) showed the feasibility and spontaneity of the adsorption process, and the adsorption capacity decreases with increasing the temperature favored at low temperature. The positive value of $\Delta H°$ (6.0449 $kJmol^{-1}$) and negative value of $\Delta S°$ (-17.335 $Jmol^{-1}K^{-1}$) confirmed the endothermic nature of the process and no change in the internal structure of the ion exchange adsorbent. The adsorbent also possesses high value of dielectric constant, dielectric loss, and high AC electric conductivity at low frequency at 30°C. The adsorbent was also used as photocatalyst that showed significant result for the photocatalytic degradation of two industrial dyes, rhodamine B and crystal violet. All these findings conclude that the applicability of polyacrylamide Zr(IV) phosphosulphosalicylate cation exchanger is not only as a potential adsorbent but also as a photocatalyst for the removal of inorganic and organic pollutant from the aqueous solution and may be used in energy storage devices. Therefore, synthesized material could be employed in miscellaneous field.

Acknowledgements The authors are thankful to Chairman, Department of Chemistry, Aligarh Muslim University, Aligarh, and also thankful to UGC (DRS-II) and DST (FIST & PURSE) for providing necessary research facilities.

References

1. Shen, X.; Wang, Q.; Chen, W.; Pang, Y.: Appl. Surf. Sci. **317**, 1028 (2014). doi:10.1016/j.apsusc.2014.09.033
2. Cui, L.; Guo, X.; Wei, Q.; Wang, Y.; Gao, L.; Yan, L.; Yan, T.; Du, B.: J. Colloid Interf. Sci. **439**, 112 (2015). doi:10.1016/j.jcis.2014.10.019
3. Chena, M.; Qin, X.; Zeng, G.; Li, J.: Impacts of human activity modes and climate on heavy metal "spread" in groundwater are biased. J. Chemos. **152**, 439–445 (2016)
4. Krishnani, K.K.; Meng, X.; Dupont, L.: Metal ions binding onto lignocellulosic biosorbent. J. Environ. Sci. Health A **44**, 688 (2009). doi:10.1080/10934520902847810
5. De, M.; Azargohar, R.; Dalai, A.K.; Shewchuk, S.R.: Mercury removal by bio-char based modified activated carbons. Fuel **103**, 570 (2013). doi:10.1016/j.fuel.2012.08.011
6. Rao, M.M.; Reddy, D.H.K.K.; Venkateswarlu, P.; Seshaiah, K.: Removal of mercury from aqueous solutions using activated carbon prepared from agricultural by-product/waste. J. Env. Manag. **90**, 634 (2009). doi:10.1016/j.jenvman.2007.12.019

7. Lu, X.; Jiang, J.; Sun, K.; Wang, J.; Zhang, Y.: Influence of the pore structure and surface chemical properties of activated carbon on the adsorption of mercury from aqueous solutions. Mar. Pol. Bul. **78**, 69 (2014). doi:10.1016/j.marpolbul.2013.11.007
8. Chen, M.; Xua, P.; Zeng, G.; Yang, C.; Huang, D.; Zhang, J.: Bioremediation of soils contaminated with polycyclic aromatic hydrocarbons, petroleum, pesticides, chlorophenols and heavymetals by composting: Applications, microbes and future research needs. Biotech. Adv. **33**, 745–755 (2015). doi:10.1016/j.biotechadv.2015.05.003
9. AL-Othman Z.A., Naushad Mu.: Inamuddin, Organic–inorganic type composite cation exchanger poly-o-toluidine Zr(IV) tungstate: Preparation, physicochemical characterization and its analytical application in separation of heavy metals, Chem. Eng. J. **172**, 369 (2011) doi:10.1016/j.cej.2011.06.018
10. Sharma, P.: Neetu, Synthesis, characterization and sorption behavior of zirconium(IV) antimonotungstate: An inorganic ion exchanger. Desalination. **267**, 277 (2011). doi:10.1016/j.desal.2010.09.040
11. Akhtar, A.; Khan, M.D.A.; Nabi, S.A.: Synthesis, characterization and photolytic degradation activity of poly-o-toluidine-thorium(IV)molybdophosphate cation exchanger: Analytical application in metal ion treatment. Desalination. **361**, 1 (2015). doi:10.1016/j.desal.2015.01.028
12. Rahman, N.; Haseen, U.; Rashid, M.: Synthesis and characterization of polyacrylamide zirconium (IV) iodate ion-exchanger: Its application for selective removal of lead (II) from wastewater. Arabian J. Chem. (2013) doi:10.1016/j.arabjc.2013.06.029
13. Rahman, N.; Haseena, U.: Development of polyacrylamide chromium oxide as a new sorbent for solid phase extraction of As(III) from food and environmental water samples. RSC Adv. **5**, 7311–7323 (2015)
14. Khan, A.A.; Shaheen, S.; Habib, U.: Synthesis and characterization of poly-o-anisidine Sn(IV)tungstate: A new and novel 'organic-inorganic'nano-composite material and its electro-analytical applications as Hg (II) ion-selective membrane electrode. J. Adv. Res. **3**, 269 (2012) doi:10.1016/j.jare.2011.09.002
15. Rahman, N.; Haseen, U.: Inorganic and Polymeric Hybrid Ion Exchangers: Removal of Toxic Heavy Metal ions. Lap Lambert Academic Publishing, Germany (2014). ISBN -13:978-3-659-38850-7)
16. Arrad, O.; Sasson, Y.: Commercial ion exchange resins as catalysts in solid-solid-liquid reactions. J. Org. Chem. **54**, 4993 (1989). doi:10.1021/jo00282a008
17. Lutfullah, Rashid M.; Rahman, N.: Zirconium(IV) Phosphosulphosalicylate as an Important Lead(II) Selective Ion-Exchange Material: Synthesis, Characterization and Adsorption Study, Adv. Sci. Lett. **17**, 184 (2012) doi:10.1166/asl.2012.3683
18. Lutfullah, Rashid M., Rahman N., Synthesis, characterization and sorption characteristics of a fibrous organic—inorganic composite material, Adv. Sci. Lett. **17**, 136 (2012) DOI:10.1166/asl.2012.3691
19. Langmuir, I.: the adsorption of gases on plane surfaces of glass, mica and platinum. J. Am. Chem. Soc. **40**, 1361 (1918). doi:10.1021/ja02242a004
20. Crini, G.: Kinetic and equilibrium studies on the removal of cationic dyes from aqueous solution by adsorption onto a cyclodextrin polymer. Dyes Pigments **77**, 415 (2008). doi:10.1016/j.dyepig.2007.07.001
21. Rahman, N.; Haseen, U.: Equilibrium modeling, kinetic, and thermodynamic studies on adsorption of Pb(II) by a hybrid inorganic-organic material: polyacrylamide zirconium(IV) iodate, Ind. Eng. Chem. Res. **53**, 8198 (2014) http://pubs.acs.org/doi/pdf/10.1021/ie500139k
22. Gupta, N.; Kushwaha, A.K.; Chattopadhyaya, M.C.: Adsorption studies of cationic dyes onto Ashoka (Saraca asoca) leaf powder. J. Taiwan Inst. Chem. Eng. **43**, 604 (2012). doi:10.1016/j.jtice.2012.01.008
23. Hameed, B.H.: Grass waste: a novel sorbent for the removal of basic dye from aqueous solution. J. Hazard. Mat. **166**, 233 (2009). doi:10.1016/j.jhazmat.2008.11.019
24. Zhao, F.; Tang, W.Z.; Zhao, D.; Meng, Y.; Yin, D.; Sillanpää, M.: Adsorption kinetics, isotherms and mechanisms of Cd(II), Pb(II), Co(II) and Ni(II) by a modified magnetic polyacrylamide microcomposite adsorbent. J. Water Process Eng. **4**, 47 (2014). doi:10.1016/j.jwpe.2014.09.003
25. Zhao, F.; Repo, E.; Yin, D.; Sillanpaa, M.E.T.: Adsorption of Cd(II) and Pb(II) by a novel EGTA-modified chitosan material: kinetics and isotherms. J. Coll. Interface Sci. **409**, 174 (2013). doi:10.1016/j.jcis.2013.07.062
26. Mane, V.S.; Mall, I.D.; Srivastava, V.C.: Kinetic and equilibrium isotherm studies for the adsorptive removal of Brilliant Green dye from aqueous solution by rice husk ash. J. Environ. Manag. **84**, 390 (2007). doi:10.1016/j.jenvman.2006.06.024
27. Atkins, P.: Physical Chemistry, 6th edn. Oxford University Press, London (1999)
28. Lagergren, S.: About the theory of so-called adsorption of soluble substances. Kungliga Svenska Vetenskapsakademiens. Handlingar **24**, 1 (1898)
29. Ho, Y.S.; McKay, G.: Pseudo-second order model for sorption processes. Process. Biochem. **34**, 451 (1999). doi:10.1016/S0032-9592(98)00112-5
30. Weber, W. J.; Morris, J. C.: J. Sani. Eng. Div. **89**, 31 (1963) http://cedb.asce.org/cgi/WWWdisplay.cgi?13042
31. Donia, A.M.; Atia, A.A.; Al-amrani, W.A.; El-Nahas, A.M.: Effect of structural properties of acid dyes on their adsorption behaviour from aqueous solutions by amine modified silica. J. Hazard. Mat. **161**, 1544 (2009). doi:10.1016/j.jhazmat.2008.05.042
32. Ahmad, A.; Rafatullah, M.; Sulaiman, O.; Ibrahim, M.H.; Hashim, R.: Scavenging behaviour of meranti sawdust in the removal of methylene blue from aqueous solution. J. Hazard. Mat. **170**, 357 (2009). doi:10.1016/j.jhazmat.2009.04.087
33. Raza, W.; Haque, M.M.; Muneer, M.; Fleisch, M.; Hakki, A.; Bahnemann, D.: Photocatalytic degradation of different chromophoric dyes in aqueous phase using La and Mo doped TiO_2 hybrid carbon spheres. J. Alloys Compd. **632**, 837 (2015). doi:10.1016/j.jallcom.2015.01.222
34. Qureshi, S.Z.; Khan, M.A.; Rahman, N.: Synthesis and ion exchange behaviour of a new three-component ion exchange material: zirconium (IV) arsenate vanadate. Bull. Chem. Soc. Jpn. **68**, 1613–1617 (1995)
35. Socrates, G.: Infrared Characteristic Group Frequencies. Wiley, New York (1980). 145
36. Nabi, S.A.; Shahadata, M.; Bushra, R.; Oves, M.; Ahmed, F.: synthesis and characterization of polyanilineZr(IV)sulphosalicylate composite and its applications (1) electrical conductivity, and (2) antimicrobial activity studies. Chem. Eng. J. **173**, 706–71 (2011)
37. Apopei, D.F.; Dinu, M.V.; Trochimczuk, A.W.; Dragan, E.S.: Sorption isotherms of heavy metal ions onto semi-interpenetrating polymer network cryogels based on polyacrylamide and anionically modified potato starch. Ind. Eng. Chem. Res. **51**, 10462 (2012). doi:10.1021/ie301254z
38. Khan, M.D.A.; Akhtar, A.; Nabi, S.A.: Kinetics and thermodynamics of alkaline earth and heavy metal ion exchange under particle diffusion controlled phenomenon using polyaniline-sn(iv)iodophosphate nanocomposite. J. Chem. Eng. Data **59**, 2677 (2014). doi:10.1021/je500523n
39. Irfan, M.; Islam, M.U.; Ali, I.; Iqbal, M.A.; Karamat, N.; Khan, H.M.: Effect of Y_2O_3 doping on the electrical transport properties of $Sr_2MnNiFe_{12}O_{22}$ Y-type hexaferrite. Cur. App. Phy. **14**, 112 (2014). doi:10.1016/j.cap.2013.10.010

40. Baral, A. K.; Sankaranarayanan, V.: Ion transport and dielectric relaxation studies in nanocrystalline $Ce_{0.8}Ho_{0.2}O_{2-\delta}$ material. Phys. B: Cond. Mater. **404**, 1674–1678 (2009) doi:10.1016/j.physb.2009.02.002
41. Baral, A. K.; Narayanan, S.; Ramezanipour, F.; Thangadurai, V.: Evaluation of fundamental transport properties of Li-excess garnet-type Li5+2xLa3Ta2xYxO12 (x = 0.25, 0.5 and 0.75) electrolytes using AC impedance and dielectric spectroscopy, Phy. Chem. Chem. Phy. **16**, 11356 (2014) DOI:10.1039/C4CP00418C
42. Khan, M.D.A.; Akhtar, A.; Nabi, S.A.: Investigation of the electrical conductivity and optical property of polyaniline-based nanocomposite and its application as an ethanol vapor sensor. New J. Chem. **39**, 3728 (2015). doi:10.1039/C4NJ02260B
43. Hashim, M.; Alimuddin, Kumar S.; Shirsath, S. E.; Kotnala, R.K.; Shah, J.; Kumar, R.: Synthesis and characterizations of Ni2þ substituted cobalt ferrite nanoparticles, Mat. Chem. Phys. **139**, 364 (2013). doi:10.1016/j.matchemphys.2012.09.019
44. Yin, H.; Yu, K.; Song, C.; Huang, R.; Zhu, Z.: Synthesis of Au-Decorated V2O5@ZnO Heteronanostructures and Enhanced Plasmonic Photocatalytic Activity, ACS Appl. Mater. Interfaces. **6**, 14851 (2014) doi:10.1021/am501549n
45. Raza, W.; Haque, M.M.; Muneer, M.: Synthesis of visible light driven ZnO: Characterization and photocatalytic performance. Appl. Surf. Sci. **322**, 215 (2014). doi:10.1016/j.apsusc.2014.10.067
46. Mukhlish, M.Z.B.; Najnin, F.; Rahman, M.M.; Uddin, M.J.: Photocatalytic degradation of different dyes using TiO_2 with high surface area: a kinetic study. J. Sci. Res. **5**, 301 (2013). doi:10.3329/jsr.v5i2.11641
47. Tang, J.; Huang, Y.; Gong, Y.; Lyu, H.; Wang, Q.; Ma, J.: Preparation of a novel graphene oxide/Fe–Mn composite and its application for aqueous Hg(II) removal. J. Hazard. Mater. **316**, 151–158 (2016). doi:10.1016/j.jhazmat.2016.05.028
48. Hadavifar, M.; Bahramifar, N.; Younesi, H.; Rastakhiz, M.; Li, Q.; Yu, J.; Eftekhari, E.: Removal of mercury(II) and cadmium(II) ions from synthetic wastewater by a newly synthesized amino and thiolated multi-walled carbon nanotubes. J. Taiwan Inst. Chem. Eng. **67**, 397–405 (2016). doi:10.1016/j.jtice.2016.08.029
49. Choi, J.M.; Jeong, D.; Cho, E.; Jun, B.; Park, S.; Yu, J.; Tahir, M.N.; Jung, S.: Chemically functionalized silica gel with alkynyl terminated monolayers as an efficient new material for removal of mercury ions from water. J. Ind. Eng. Chem. **35**, 376–382 (2016). doi:10.1016/j.jiec.2016.01.020
50. Shafiabadi, M.; Dashti, A.; Tayebi, H.: Removal of Hg (II) from aqueous solution using polypyrrole/SBA-15 nanocomposite: Experimental and modeling. Synth. Meter. **212**, 154–160 (2016). doi:10.1016/j.synthmet.2015.12.020
51. Yao, X.; Wang, H.; Ma, Z.; Liu, M.; Zhao, X.; Jia, D.: Adsorption of Hg(II) from aqueous solution using thiourea functionalized chelating fiber, Chin. J. Chem. Eng. (2016)
52. Kumara, A. S. K.; Jiang, S.; Tseng, W.: Facile synthesis and characterization of thiol-functionalized graphene oxide as effective adsorbent for Hg(II), J.Env. Chemi. Eng. **4**, 2, 2052–2065 (2016) http://www.sciencedirect.com/science/article/pii/S2213343716301130#articles
53. Liu, L.; Ding, L.; Wu, X.; Deng, F.; Kang, R.; Luo, X.: Enhancing the Hg(II) removal efficiency from real wastewater by novel thymine-grafted reduced graphene oxide complexes. Ind. Eng. Chem. Res. **55**, 6845–6853 (2016). doi:10.1021/acs.iecr.6b01359